

Article

Soil Loss Potential Assessment for Natural and Post-Fire Conditions in Evia Island, Greece

Kanella Valkanou ¹, Efthimios Karymbalis ^{1,*}, George Bathrellos ², Hariklia Skilodimou ²,
Konstantinos Tsanakas ¹, Dimitris Papanastassiou ³ and Kalliopi Gaki-Papanastassiou ⁴

¹ Department of Geography, Harokopio University, 70 El. Venizelou Str., GR-17671 Athens, Greece

² Department of Geology, University of Patras, GR-26504 Rio Patras, Greece

³ Institute of Geodynamics, National Observatory of Athens, GR-11810 Athens, Greece

⁴ Department of Geography and Climatology, Faculty of Geology and Geoenvironment, University of Athens, GR-15784 Athens, Greece

* Correspondence: karymbalis@hua.gr

Abstract: A devastating forest fire in August 2021 burned about 517 km² of the northern part of Evia Island, affecting vegetation, soil properties, sediment delivery and the hydrological response of the catchments. This study focuses on the estimation of the annual soil loss in the study area under natural (pre-fire) and post-fire conditions. The assessment of the soil loss potential was conducted with the application of the Universal Soil Loss Equation (USLE), which is an empirical equation and an efficient way to predict soil loss. The USLE factors include rainfall erosivity (R), soil erodibility (K), the slope and slope length factor (LS), the cover management factor (C) and the erosion control practice factor (P). The USLE quantified the annual soil erosion (in t/ha/year) for both pre- and post-wildfire conditions, and the study area has been classified into various soil loss categories and soil erosion intensity types. The results showed that the annual soil loss before the forest fires ranged from 0 to 1747 t/ha, with a mean value of 253 t/ha, while after the fire the soil loss significantly increased (the highest annual soil loss was estimated at 3255 t/ha and the mean value was 543 t/ha). These values demonstrate a significant post-fire change in mean annual soil loss that corresponds to an increase of 114% compared to the pre-fire natural condition. The area that is undergoing high erosion rates after the extreme wildfire event increased by approximately 7%, while the area of moderate rates increased by 2%. The calculated maximum potential of soil erosion, before and after the 2021 extreme wildfire event, has been visualized on spatial distribution maps of the average annual soil loss for the study area. The present study underlines the significant post-fire increase in soil loss as part of the identification of the more vulnerable to erosion areas that demand higher priority regarding the protective/control measures.

Keywords: soil loss; soil erosion risk; USLE (Universal Soil Loss Equation); GIS (Geographic Information System); post-fire effects; northern Evia Island; Central Greece



Citation: Valkanou, K.; Karymbalis, E.; Bathrellos, G.; Skilodimou, H.; Tsanakas, K.; Papanastassiou, D.; Gaki-Papanastassiou, K. Soil Loss Potential Assessment for Natural and Post-Fire Conditions in Evia Island, Greece. *Geosciences* **2022**, *12*, 367. <https://doi.org/10.3390/geosciences12100367>

Academic Editors: Deodato Tapete, Francesca Cigna, Luis Cea and Jesus Martinez-Frias

Received: 28 July 2022

Accepted: 28 September 2022

Published: 1 October 2022

Publisher's Note: MDPI stays neutral with regard to jurisdictional claims in published maps and institutional affiliations.



Copyright: © 2022 by the authors. Licensee MDPI, Basel, Switzerland. This article is an open access article distributed under the terms and conditions of the Creative Commons Attribution (CC BY) license (<https://creativecommons.org/licenses/by/4.0/>).

1. Introduction

Soil erosion can be described as the removal and transportation of soil particles from the surface of the earth by the action of water and wind under the influence of gravity [1]. When this geomorphic process is accelerated by several human activities, such as deforestation, land development, overexploitation, constructions and other physical environmental interventions, it can become a natural hazard, causing long-term negative effects. The natural resources of land and water, as well as their interdependence and interactions, ensure life on earth [2], while their degradation undermines human development and life quality. Water erosion also threatens biodiversity. Orgiazzi and Panagos [3] developed a biological factor to be incorporated in their soil erosion modeling because of this connection. However, Stefanidis et al. [4] suggest that this relationship is reciprocal. Soil erosion has

been classified among the most severe natural hazards worldwide [5] that threatens the soil resources globally [6].

Among the European countries, the Mediterranean ones host the most susceptible to soil erosion areas [7,8], mainly because of natural factors such as the climatic conditions, the rough relief and the soil properties, which intensify erosional processes. When these natural factors interact with the anthropogenic influence, the result is higher rates of soil erosion with crucial environmental and socio-economic impacts [8].

The quantification of the soil erosion potential is necessary to ensure the safe and sustainable development of an area [9]. The estimation of soil loss potential is also particularly useful for scientists, planners, and decision makers to coordinate mitigation measures and effective strategies, especially in areas that are being affected by forest fires of high severity. Surface runoff and soil erosion rates are expected to be significantly higher in burned areas [10–12]. Thus, the assessment of soil loss is considered necessary to evaluate the potential future risk, to identify erosion impacts on the environment, as well as to design reconstruction plans [13] that prevent further deterioration of the soil. Among the emergency post-fire erosion mitigation works mainly applied in Greece are hillslope rehabilitation treatment of contour-felled logs, branch piles [14], erosion barriers, mulch, chemical treatments [15] and a total ban on grazing [16].

It has been frequently reported that the first year after a forest fire, the hydrologic response and the sediment production increase several times when compared with the pre-fire condition [9,17–21]. Among the most important factors that affect surface runoff and erosion, after the occurrence of wildfires, are the severity and frequency of the fire, the magnitude and intensity of the rainfall, the soil properties, and especially soil moisture that is significantly altered after the fire, and the land cover changes [18].

Although fire effects on the response of the drainage systems as well as on the soil erosion potential are important, fire-related issues are quite complex. To guide right decisions for the mitigation of soil loss and degradation, it is necessary to accurately predict the post-fire effects and to make precise estimations of the expecting surface runoff and sediment production [19]. Several models and approaches have been proposed for the assessment of the soil loss potential at both global and European scales. The technological boost that enhanced Geographic Information Systems (GIS) has positively contributed to the evolution of new procedures. These are either expert-based methods or model-based approaches, such as the one used in the current study. Over the last years, many papers have explored the factors controlling soil erosion [22,23], while others focus on the assessment of post-fire erosion rates with the use of several methodologies [18,24–27] or analyze and discuss the effectiveness of the post-fire mitigation treatments [27–29]. The majority of these approaches include quantitative geomorphometric analyses [29,30], the application of GIS and remote sensing techniques [31–33], the use of empirical equations [12,34,35], the combination of fuzzy logic and analytic hierarchy processes [36–38] and the use of integrated methods that incorporate different data to computational tools [38–41].

Regarding the soil erosion studies in Greece, van Andel et al. [42] investigated the extent of soil erosion and the dominant control of land use on soil loss during the prehistoric and historic eras, while the study of Zangger [43] provided evidence in support of a human cause of deforestation and soil erosion at the transitional period known as the Final Neolithic-Early Bronze Age. Over the last years, several studies have been conducted on soil erosion assessment, as well as on prevention measures. Many of them have been systematically discussed by the representative review paper by Koutalakis et al. [44], whereas the paper of Schismenos et al. [45] presents the soil governance in Greece.

Concerning Evia Island, Rozos et al. [46] applied the RUSLE model and they compared the prone to soil erosion areas with the recorded landslides, and their results showed a satisfactory correlation. The same prediction model was also used by Stefanidis et al. [4] to quantify the effects of the 2021 wildfires on soil erosion dynamics for multiple fire-affected areas of Greece, with the study area being one of the case studies. Evelpidou et al. [47] applied the Boolean logic-based model in an attempt to assess the effects of the wildfires

on the susceptibility of the study area to surface runoff erosion, and the results suggested that the area is highly susceptible to near-future erosion events.

The aim of this paper is to assess the soil loss potential in the northern part of Evia Island (Central Greece) both before and after the devastating forest fire event of 2021. The estimation was performed with the use of the simple, robust and widely applied Universal Soil Loss Equation (USLE) [48] in a GIS environment. This is the first attempt of soil erosion potential assessment with the application of the USLE methodology in the study area. The mean and maximum annual average soil loss values under natural (pre-fire) and post-fire conditions were estimated and compared, while predictive spatial distribution soil erosion maps were compiled based on the input factors. The analysis allowed us to assess the soil erosion level not only within the northern part of Evia but also separately for the burned sub-region, indicating the areas of priority regarding the erosion control measures that are required to be taken.

2. Study Area

The study area is the northern part of Evia Island, located in Central Greece, and covers an area of 1842.3 km² (Figure 1). Evia, the second-largest Greek island, has an elongated shape with a NW–SE direction. The northern part of the island lies between the Aegean Sea to the northeast and the north Gulf of Evia to the southwest, while to the north it is separated from the mainland by the Oreos-Trikeri straits (Figure 1).

In terms of geotectonics, it belongs to the rapidly extending region of the Aegean Sea, and the tectonic pattern of the area is reflected in the landscape [49,50]. Its landscape is characterized by a sequence of mountain ridges and low-lying plains and reflects the tectonic pattern of the area [50,51]. The highest altitude is the peak of Dirfis Mountain (1736.8 m), located at the southeastern part of the study area. Lithologically, the study area consists of carbonate rocks, ophiolites, schists, cherts, marls, and sandstones, while alluvial deposits occur along the major channels of the drainage networks as well as at the mouth of the rivers [52].

The study area belongs to the continental and lowland Mediterranean climate types, with drier summers and colder winters, while the highland Mediterranean climate is found at the high mountain ranges [53–55]. Mean annual rainfall ranges between 400 and 1100 mm, while mean annual air temperature fluctuates between 4 and 22 °C.

During the peak of the traditional fire season, in August 2021, Greece suffered from severe and extensive wildfires, with significant direct impacts on humans, economy, environment and ecosystems, also causing alterations of soil properties. According to Giannaros et al. [56], this was the worst fire season of the past 13 years since an area of approximately 94000 ha, including part of the northern Evia Island, has been totally burned. The forest fire that affected the study area is considered the largest in the recent Greek history since it impacted an area of approximately 517 km² and destroyed in total more the 400 km² of forest [57] (Figure 1). A major part of the burned area was forestland of exceptional natural beauty and agricultural land. Since the main sources of income for most of the inhabitants were honey and pine-resin production (both depended on forest) [57], agricultural products and tourism, the local economy was dramatically affected. The ecosystems of Evia Island have suffered many wildfires in a short period of 10 years, according to the Copernicus Emergency Management Service [58], and therefore the pinewood ecosystem is impossible to naturally regenerate since the nutrient depletion is extensive [59].

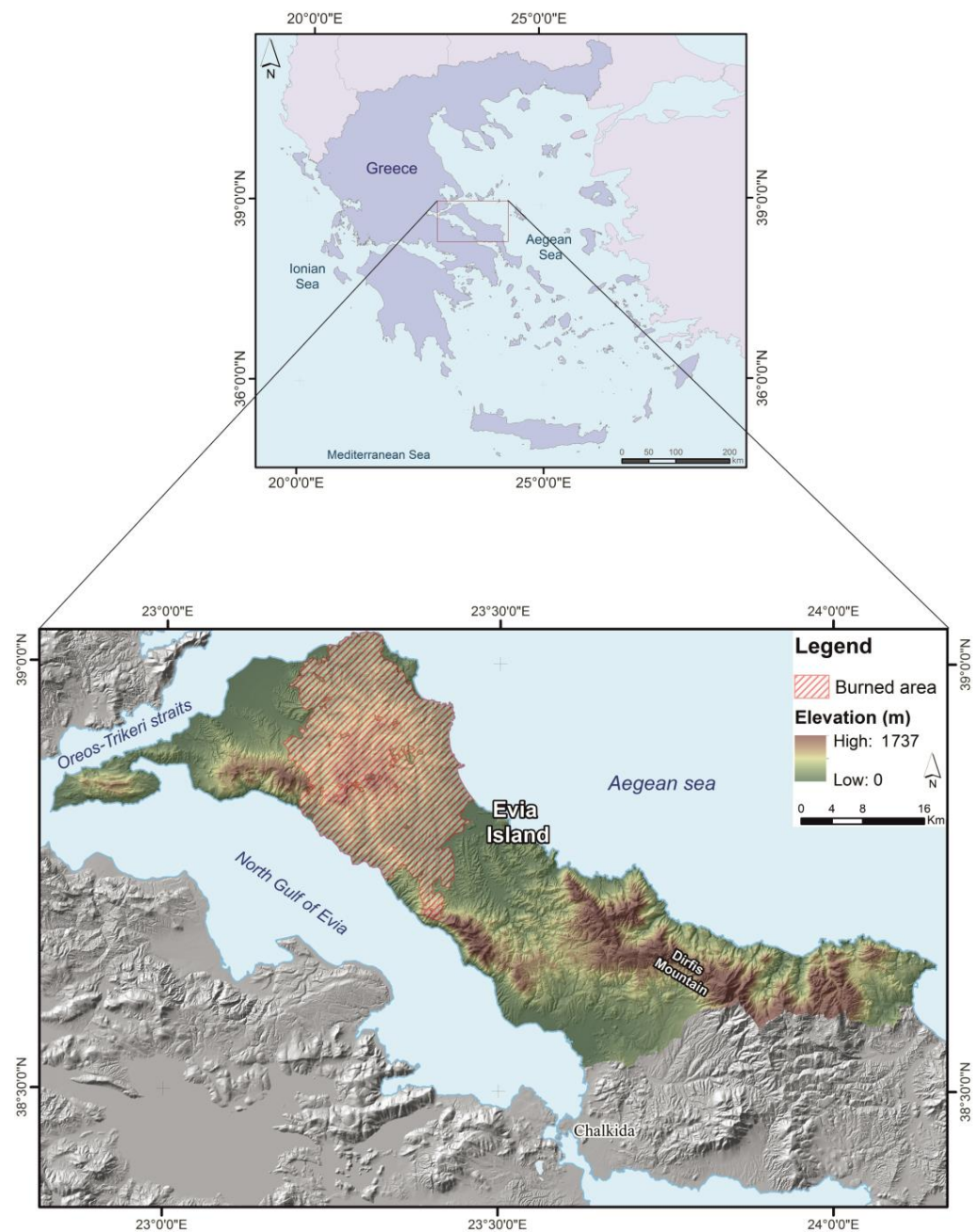


Figure 1. Digital Elevation Model (DEM) of the northern part of Evia Island, showing the location of the study area. The hatched polygon represents the burned area following the August 2021 wildfire event.

3. Materials and Methods

3.1. The Universal Loss Equation

The USLE is a simple empirical equation for the prediction of long-term soil loss (in tons per hectare per year) due to erosional processes as a function of five factors [48], and can be calculated as shown in the following Equation (1):

$$A = R \times K \times LS \times C \times P \quad (1)$$

where A = average annual soil loss rate (t/ha/year), R = rainfall erosivity factor ($\text{MJ} \times \text{mm}/\text{ha}/\text{h}/\text{year}$), K = soil erodibility factor ($\text{t} \times \text{ha} \times \text{h}/\text{ha}/\text{MJ}/\text{mm}$),

LS = topographic factor (unitless), C = cropping management factor (unitless) and P = erosion control practice factor (unitless).

After the estimation of each of the factors, the factor layers were imported in a GIS database and the USLE equation was calculated. In this way, raster maps of soil erosion potential were generated, and then annual soil loss values were calculated for the study area under both natural and post-fire conditions. The study area was classified into three groups of erosion intensity (the low erosion level class with soil loss values less than 9 t/ha/year, the moderate erosion level class with soil loss values between 10 and 36 t/ha/year and the high to extremely high level class with values higher than 37 t/ha/year) and changes in soil loss potential because of the forest fires were estimated. Moreover, calculations regarding the erosion level were implemented for the burned, after the 2021 wildfire, sub-area. A schematic representation of the methodology followed is presented in Figure 2.

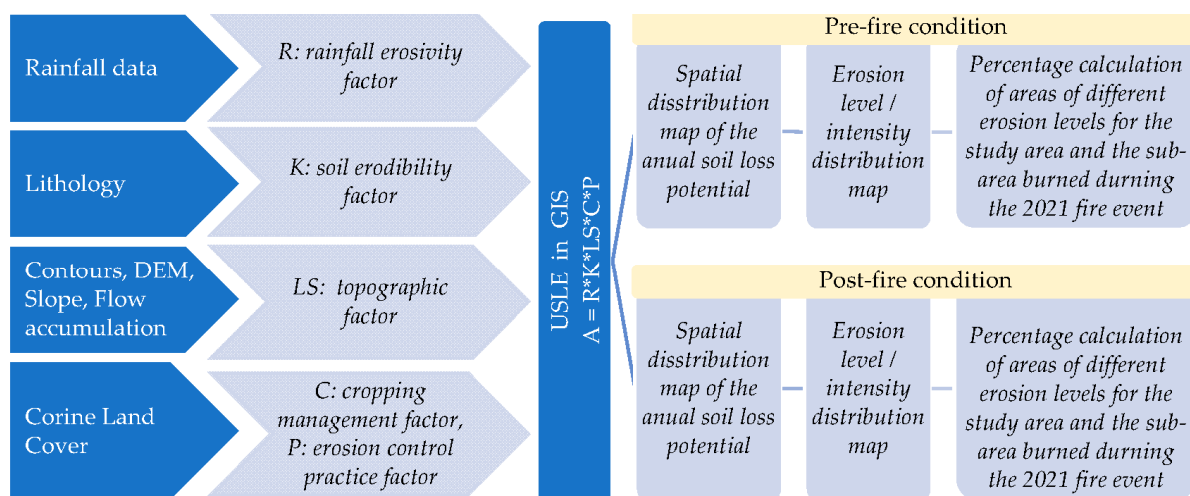


Figure 2. Schematic representation of the methodology employed.

The data used for the estimation of the USLE factors are summarized in the following paragraphs.

3.2. Data

All the calculations were performed utilizing ArcGIS software and were based on raster files with a cell size of 25×25 m. These raster files were produced from primary layers of a spatial geo-database designed and implemented for the purposes of this study. Data processing included several steps to adjust the variables to the input requirements. The vector data were either downloaded from open-source datasets (the Corine database) or were derived through digitization from raster maps. The data used were:

- Topographic maps of the study area at a 1:50000 scale, published by the Hellenic Military Geographical Service (HMGS).
- EU-DEM 25 m, source: "Copernicus" Land Monitoring Service.
- Geological maps at a 1:50000 scale, published by the Institute of Geology and Mineral Exploration of Greece (IGME), which were used to digitize the boundaries of the geological formations.
- The Climatic Atlas of Greece (1971–2000) developed by the Hellenic National Meteorological Service (HNMS), which was used to digitize the precipitation zones of the study area.
- The CORINE database (Corine Land Cover at scale 1:100000) downloaded by the Hellenic Mapping and Cadastral Organization, which provided the geographic distribution of individual land use classes.

3.3. Estimation of the USLE Factors

3.3.1. Rainfall Erosivity Factor (R)

For the calculation of the rainfall erosivity factor (R), rainfall (total storm energy) and rainfall intensity (maximum 30-min intensity) measurements are required. However, such measurements are usually unavailable for common meteorological stations. Hence, for the calculation of R, we used the following Equation (2), which is generally considered to be suitable for Europe [60]:

$$R = a \times P_j \quad (2)$$

where P_j = annual rainfall (mm) based on the Climatic Atlas of Greece (classes are shown in Table 1), and coefficient $a = 1.1$ to 1.5 (1.3 is the most frequently used value) [60].

Table 1. Zones of annual rainfall (in mm) for the study area.

Zones	Rainfall (mm)
1	400–500
2	500.001–600
3	600.001–700
4	700.001–1100

There is a direct correlation between factor R and soil loss since high rates of rainfall increase surface runoff, resulting in higher soil erosion rates [61].

3.3.2. Soil Erodibility Factor (K)

For the calculation of the soil erodibility factor (K), a large amount of soil properties' data is needed. Since this kind of data is not available for Greece, we used the geological formations of the study area after their classification into four groups based on their sensitivity to erosion [51]. The K factor values assigned to each group of the geological formations of the study area (Table 2) were based on the values proposed in similar approaches for the southern part of Evia Island [62].

Table 2. Soil erodibility (K) factor values for the four classes of the geological formations of the study area.

Group of Formations	K Factor Value
Group 1 (alluvial deposits, recent talus cones and scree)	0.02
Group 2 (marls, sandstones, schists, cherts and travertines)	0.012
Group 3 (schists and phyllites)	0.009
Group 4 (limestones, dolomites, greywackes, consolidated conglomerates, peridotites and quartzites)	0.0005

3.3.3. Topographic Factor (LS)

The topographic factor (LS) expresses the way topography affects erosion. It is comprised of the slope length (L) and the slope steepness (S), which are calculated according to the Equations (3) and (4) [63], respectively:

$$L = 1.4 \times \{(\text{flow accumulation} \times \text{cell size})/22.13\}^{0.4} \quad (3)$$

$$S = (\sin\beta/0.0896)^{1.3} \quad (4)$$

where flow accumulation is estimated from the DEM, cell size = 25×25 m and β = slope angle in degrees estimated from the 25 m resolution DEM.

3.3.4. Cropping Management Factor (C)

The cropping management factor (C) is related to the vegetation cover. The classes used in this study (Table 3) are shown in the CORINE land cover database and are based

on the relative tables for land cover in Greece [62]. This factor determines the difference in the soil loss potential under natural and post-fire conditions.

Table 3. Cropping management factor (C) values for the land cover classes of the study area.

Land Cover	C Factor Value
Scattered urban development, beaches, sand dunes, coastal or inland marshes, industrial or commercial zones and port zones	0
Coniferous forest, mixed forest and broadleaf forest	0.001
Transitional wooded scrublands and sclerophyllous vegetation	0.009
Natural Pastures, grasslands and shrubs	0.01
Complex cultivation patterns	0.17
Land occupied by agriculture with significant areas of natural vegetation	0.2
Non-irrigated arable land	0.25
Areas of sparse vegetation	0.35
Olive groves	0.4
Mining sites	0.45
Burned areas	0.55

3.3.5. Erosion Control Practice Factor (P)

The erosion control practice (P) factor refers to the effects of implementing practices to reduce soil loss. The value of 1.0 was assigned to the P factor because it was impossible to take into consideration data of supporting practices on the scale of the present study.

4. Results and Discussion

This study focused on the calculation of the soil erosion potential and the identification of critical areas for soil conservation measures. For this purpose, the annual soil loss was estimated with the use of USLE that multiplies five determinant factors. The maps of the spatial distribution of the USLE factors' values are depicted in Figure 3a–e. Additionally, maps of both soil loss potential and erosion intensity were constructed for the study area, as well as for the sub-area burned after the 2021 mega fire.

The R factor ranges from 585 to 1170 MJ \times mm/ha/h/year, with a mean value of 828.75 MJ \times mm/ha/h/year and a standard deviation value of 217.41 MJ \times mm/ha/h/year. The highest values are in line with the high-altitude areas and are concentrated mainly at the southern and northern parts of the study area (Figure 3a). It should be noted that the burned area receives high levels of precipitation and therefore is characterized by high R factor values.

The K factor varies from 0.0005 to 0.02 t \times ha \times h/ha/MJ/mm. Its higher values are identified at the mouth of the rivers as well as on both sides along the major main channels of the drainage networks. The geological formations with the highest K factor value (0.02) cover an area of 261 km² (which corresponds to 14% of the study area), while an extensive area of 780 km² (42% of the study area) is occupied by the formations of the lowest K value. The formation with a K factor of 0.012 covers approximately 33% of the study area (Figure 3b).

The LS factor ranges from 0 to 742. The mean value is 198.76, while the standard deviation is 13.777. The major part (approximately 93%) of the study area is dominated by low values of the LS factor (<25), whereas the highest values are concentrated along the mountain ranges (Figure 3c).

The C factor ranges from 0 to 0.55. The highest values of the C factor for the pre-fire/natural condition correspond to the low-lying plains (Figure 3d), whereas for the post-fire condition the higher values correspond to the burned area (Figure 3e). Before the 2021 forest fire, approximately 32% (587 km²) of the study area was occupied by various types of forests (coniferous, mixed and broadleaf), while an equal area of 586 km² (which corresponds to 32% of the study area) was covered by transitional wooded scrublands and sclerophyllous vegetation, and 246 km² (about 13% of the study area) consisted of agricultural land with significant parts of natural vegetation. The rest (23%) of the study

area (421 km²) is occupied by other land cover types, each of which corresponds to <10% of the study area. After the fire that burned 28% of the study area (517 km²), approximately 22% of the study area is occupied by various types of forests (coniferous, mixed and broadleaf) (397 km²), while an area of 462 km² (which corresponds to 25% of the study area) is covered by transitional wooded scrublands and sclerophyllous vegetation. The rest (25%) of the study area (464 km²) is occupied by other land cover types, with each of them covering a small percentage (<10%) of the study area.

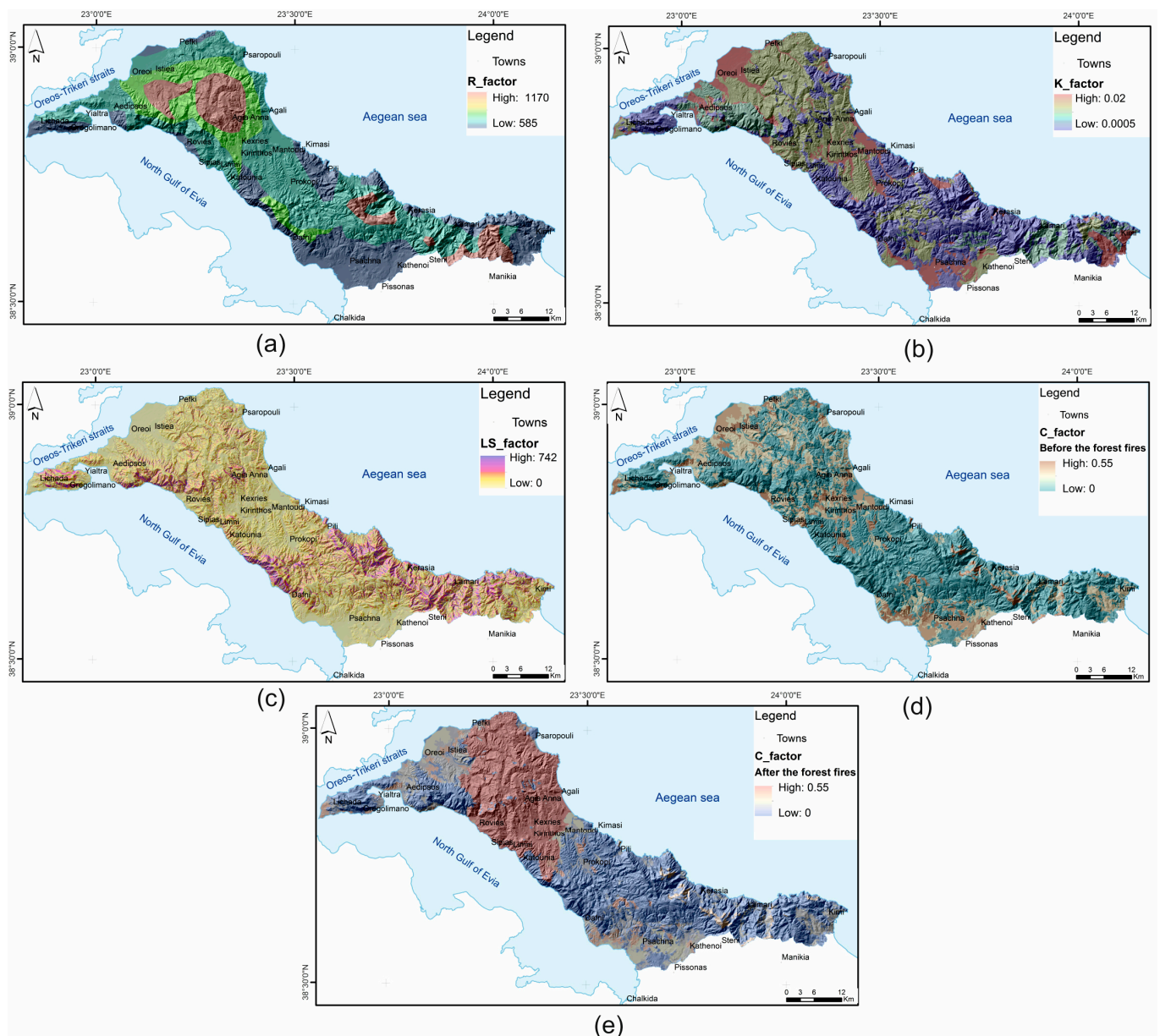


Figure 3. Spatial distribution maps of the USLE factors for the study area. (a) Rainfall erosivity (R), (b) soil erodibility (K), (c) slope length and steepness (LS), (d) cropping management (C) factor before the forest fires and (e) cropping management factor (C) after the 2021 forest fire.

The spatially distributed raster data that correspond to the above factors were integrated/multiplied, with the use of GIS tools, for different cropping management factors indicative of natural (before the fire) and post-fire conditions. The distributions of the annual soil loss potential in the northern part of Evia Island are depicted in the maps of Figures 4 and 5. The annual soil loss ranges from 0 to 1747 t/ha/year for the pre-fire

condition, while for the post-fire condition the maximum annual soil loss value reaches 3255 t/ha/year. A mean erosion rate of 253 t/ha was estimated under the natural (pre-fire) condition, which increased to 543 t/ha for the disturbed condition after the fire.



Figure 4. Spatial distribution map of the annual soil loss potential under the natural (pre-fire) condition.

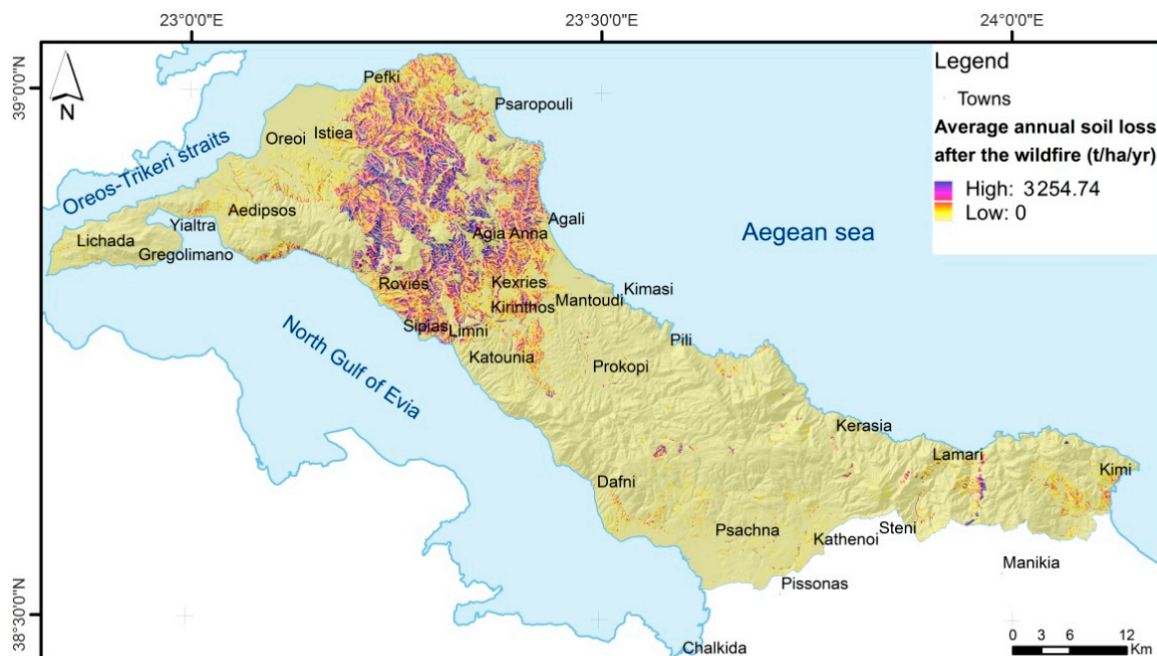


Figure 5. Spatial distribution map of the calculated annual soil loss potential under the post-fire condition.

To determine the intensity of soil loss (or erosion potential severity), the estimated soil erosion prediction was further classified into three classes. Thus, the study area was categorized into: the negligible to low erosion level class, with soil loss values less than 9 t/ha/year, the moderate erosion level class, with soil loss values between 10 and

36 t/ha/year, and the high to extremely high erosion level class of soil loss values higher than 37 t/ha/year (Figure 6a,b).

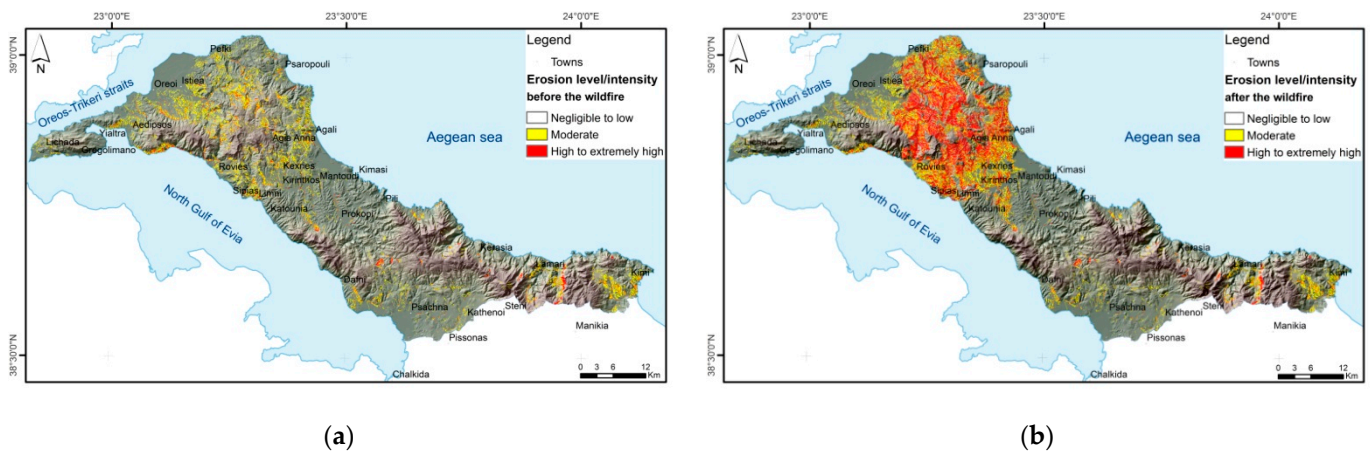


Figure 6. Erosion level maps of the study area under the (a) natural/pre-fire condition and (b) post-fire condition.

The results of the application of the USLE methodology indicate that the maximum average annual soil loss before the forest fire event of 2021 amounts to 1747 t/ha/year. However, an area of 23.24 km², which corresponds to only 1% of the study area, has values greater than 37 t/ha/year. Hence, under the natural condition, 93% of the study area is classified as of a negligible to low erosion level, 6% as moderate and the rest (1%) as of a high to extremely high erosion level (Figure 7a). The soil loss potential in the study area after the recent forest fire is calculated as significantly higher. The maximum average annual soil loss amounts to 3255 t/ha/year, with 149.76 km² (approximately 8% of the study area) having values higher than 37 t/ha/year. Thus, under the post-fire condition, 84% of the study area is classified as of a negligible to low erosion level, 8% as moderate and the rest (8%) as of a high to extremely high erosion level (Figure 7b).

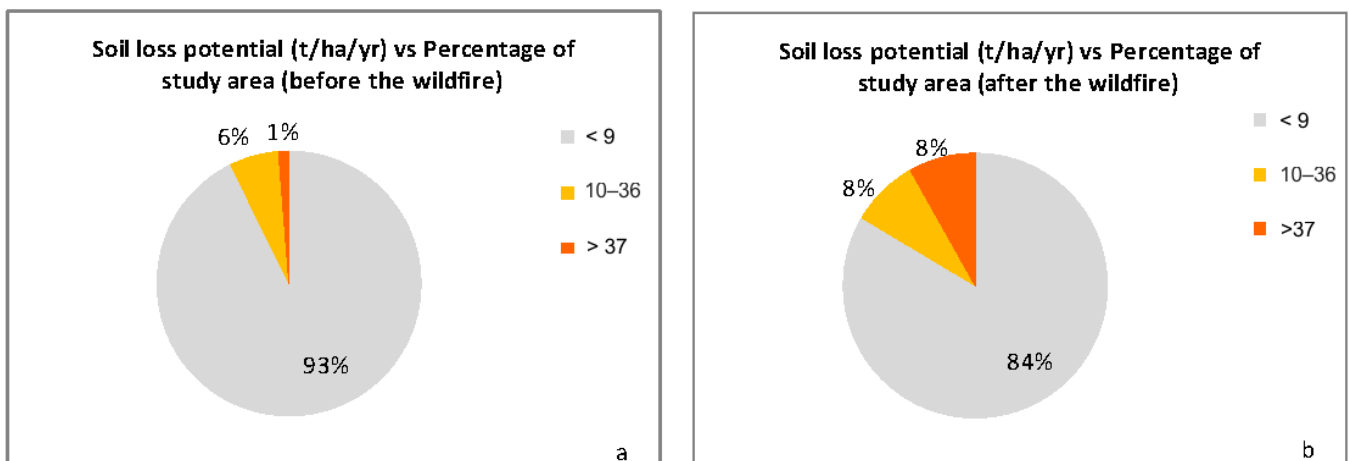


Figure 7. Soil loss potential for the total study area (a) before the wildfire and (b) after the wildfire.

At the southeastern and southwestern parts of the study area, morphological discontinuities seem to play an important role in the spatial distribution of the soil loss intensity. It is obvious that areas which are no longer protected by vegetation, after the devastating fire of 2021, experience the highest erosion rates.

The assessment of soil loss potential and the identification of the areas most likely to be subjected to maximum soil erosion are important and must be considered to design

appropriate strategies to prevent or manage the soil erosion hazard and its intensification due to forest fires.

Focusing on the burned area, the results showed that under the natural condition (if no fire had occurred), 2% of the total burned area is classified as of a high to extremely high erosion level, 11% is considered as of a moderate erosion level, while 87% presents a low erosion level (Figure 8a). On the contrary, under the post-fire condition, 26% of the burned area is classified as having a high to extremely high erosion level, 19% is classified as of a moderate erosion level, and 54% is characterized by a low erosion level (Figure 8b). This increase in the post-fire erosion level results from the significant influence of the land use change on the land degradation that causes extensive soil erosion, which in turn threatens the local communities. The spatial distribution of the erosion level for the area burned in 2021 for the pre-fire condition is depicted in Figure 9a, while for the post-fire condition in Figure 9b.

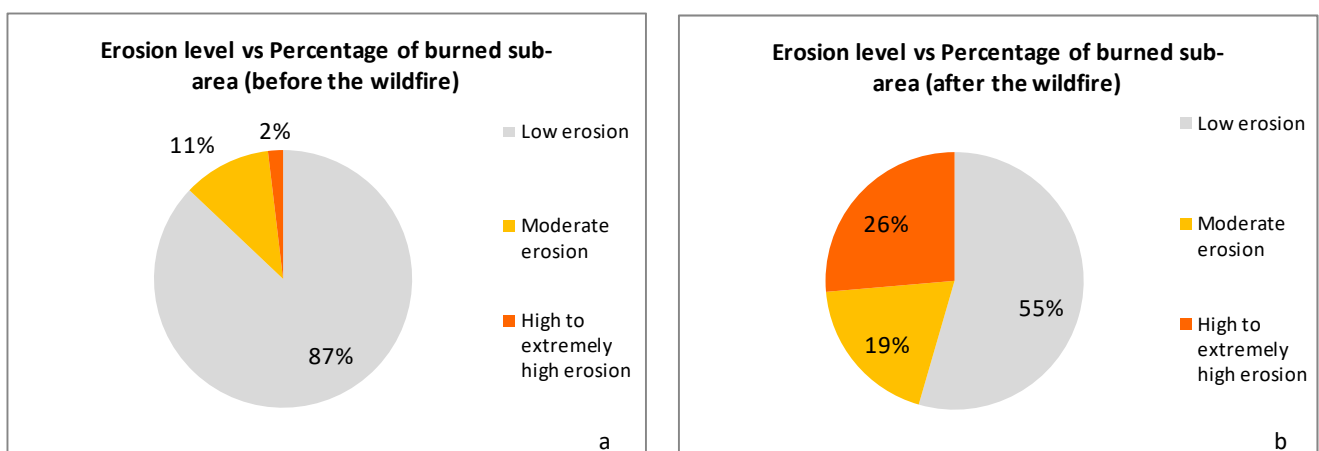


Figure 8. Erosion level for the fire-affected sub-area (a) before the wildfire and (b) after the wildfire.

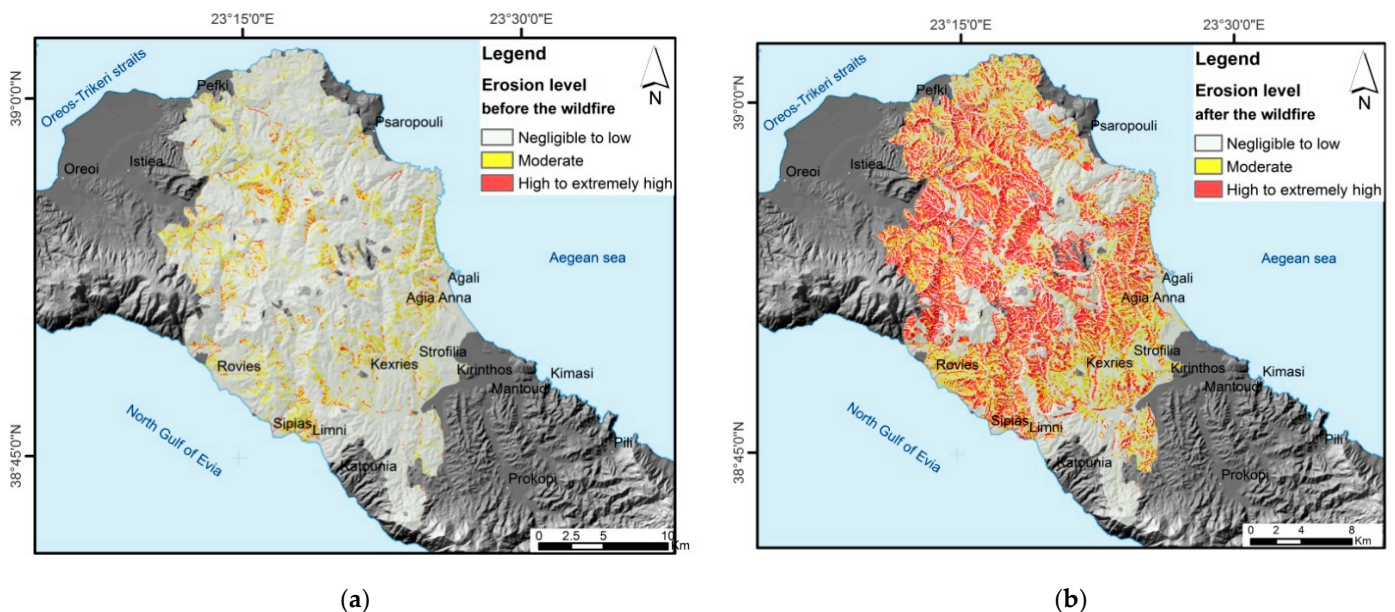


Figure 9. Erosion level mapping in the fire-affected sub-area (a) before the wildfire and (b) after the wildfire.

The results showed that after the fire, 16% of the total study area, and 45% of the area burned after the 2021 fire, were classified under moderate to high soil loss potential classes and require immediate soil conservation measures and actions. These areas of high

soil erosion risk are depicted on the map of the spatial distribution of soil loss potential after the wildfire (Figures 5 and 6b). In this context, the calculations performed may guide interventions and best management practices at different levels. This work demonstrates the usage of hazard maps in urban development and may be utilized in land use and hazard mitigation planning [64–66].

The final spatial distribution of the predicted erosion-prone areas of the post-fire condition is in good agreement with the erosion risk map prepared by Evelpidou et al. [47] using a Boolean logic-based model that considers land use, slope, lithology and drainage density. Additionally, the final spatial distribution of the predicted prone to erosion areas for the pre-fire condition is in line with both the historical slope failures map and the soil erosion map of the study area prepared by Rozos et al. [46] using the RUSLE model. The predicted areas of high soil erosion risk coincide with locations where the existence of geomorphological features indicative of erosion (such as gullies, rills, local failures in valleys and debris flows) have been identified in the field (Figure 10). Focusing on the burned sub-area, the results of this study were compared with the calculations of erosion rates proposed by Stefanidis et al. [4] using the RUSLE model and Earth observation data. The comparison demonstrates a satisfactory agreement regarding the shift from a low to a moderate–high erosion level after the recent fire, and the results of the soil loss calculations for the pre-fire condition show good accordance between the two studies.



Figure 10. Field observations showing soil erosion (a) south of Pili village and (b) north of Limni village.

5. Conclusions

This study focused on the assessment of the soil loss potential and its spatial distribution in the northern part of Evia Island based on the application of the USLE equation utilizing GIS techniques. The calculations were performed for both natural (pre-fire) and post-fire conditions.

The majority of the study area before the forest fire of 2021 was classified as of negligible to low erosion potential, and only 6% and 1% were categorized as of moderate and high erosion potential, respectively. However, after the forest fire, the area of high to extremely high erosion increased by 127 km² (which corresponds to approximately 7% of the study area), while a smaller increase by 2% was observed for the area that belongs to the class of a moderate degree of erosion. The maximum soil loss in t/ha/year within the study area increased to 86% because of the devastating recent forest fire, mainly because of the lack of forested areas. The mean soil loss potential of the post-fire condition increased by 114% compared to the pre-fire natural condition.

The results demonstrate the crucial role of the cropping management factor in the soil loss potential and revealed that vegetation cover along with rainfall erosivity and high slope are the factors that determine the soil loss in the study area.

Our approach identified the most vulnerable to erosion areas that need soil conservation management and/or interventions by priority. Such actions are required to reduce the magnitude of the post-fire erosion, the surface runoff as well as the related secondary effects.

Since increased sediment load reduces the carrying capacity of the drainage network and enhances the severity of flood events, the identification of critical erosion-prone areas for early land and water management is considered vital.

The results of this approach are in good agreement with the findings of previously conducted similar studies for the northern part of Evia Island. Future field work and efforts to collect field data by means of measurements on average soil erosion could be useful for the validation of our estimations as well as for the evaluation of the prediction's robustness.

Author Contributions: Conceptualization, K.V. and E.K.; methodology, K.V. and E.K.; formal analysis, K.V., E.K., K.T., G.B. and H.S.; data curation, K.V.; writing—original draft preparation, K.V., E.K., G.B., H.S., K.T., D.P. and K.G.-P.; writing—review and editing, K.V., E.K., G.B., H.S., K.T., D.P. and K.G.-P. All authors have read and agreed to the published version of the manuscript.

Funding: This research received no external funding.

Institutional Review Board Statement: Not applicable.

Data Availability Statement: Data are available upon request.

Acknowledgments: We would like to thank the Editors of the Journal and the anonymous reviewers for their suggestions that significantly improved the paper.

Conflicts of Interest: The authors declare no conflict of interest.

References

- Montgomery, D.R. Soil erosion and agriculture sustainability. *Proc. Natl. Acad. Sci. USA* **2007**, *104*, 13268–13272. [\[CrossRef\]](#)
- Haokip, P.; Khan, M.A.; Choudhari, P.; Kulimushi, L.C.; Qaraev, I. Identification of erosion-prone areas using morphometric parameters, land use land cover and multi-criteria decision-making method: Geo-informatics approach. *Environ. Dev. Sustain.* **2022**, *24*, 527–557. [\[CrossRef\]](#)
- Orgiazzi, A.; Panagos, P. Soil biodiversity and soil erosion: It is time to get married Adding an earthworm factor to soil erosion modeling. *J. Macroecology* **2018**, *27*, 1155–1167. [\[CrossRef\]](#)
- Stefanidis, S.; Alexandridis, V.; Spalevic, V.; Mincato, R. Wildfire Effects on Soil Erosion Dynamics: The Case of 2021 Megafires in Greece. *J. Agric. For.* **2022**, *68*, 49–63. [\[CrossRef\]](#)
- Polykretis, C.; Alexakis, D.D.; Grillakis, M.G.; Manoudakis, S. Assessment of Intra-Annual and Inter-Annual Variabilities of Soil Erosion in Crete Island (Greece) by Incorporating the Dynamic “Nature” of R and C-Factors in RUSLE Modeling. *Remote Sens.* **2020**, *12*, 2439. [\[CrossRef\]](#)
- Kadam, A.K.; Jaweed, T.H.; Kale, T.H.; Umrikar, B.N.; Sankhua, R.N. Identification of erosion-prone areas using modified morphometric prioritization method and sediment production rate: A remote sensing and GIS approach. *Geomat. Nat. Hazards Risk* **2019**, *10*, 986–1006. [\[CrossRef\]](#)
- Cerdan, O.; Desprats, J.-F.; Fouché, J.; Le Bissonnais, Y.; Chevion, B.; Simonneaux, V.; Raclot, D.; Mouillot, F. Impact of global changes on soil vulnerability in the Mediterranean Basin. Proceeding of the International Symposium on Erosion and Landscape Evolution (ISELE), Anchorage, Alaska, 18–21 September 2011; pp. 495–503. [\[CrossRef\]](#)
- Aiello, A.; Adamo, M.; Canora, F. Remote sensing and GIS to assess soil erosion with RUSLE3D and USPED at river basin scale in southern Italy. *CATENA* **2015**, *131*, 174–185. [\[CrossRef\]](#)
- Ahmed, F.; Srinivasa, R.K. Geomorphometric Analysis for Estimation of Sediment Production Rate and Run-off in Tuirini Watershed, Mizoram, India. *Int. J. Remote Sens. Appl.* **2015**, *5*, 67. [\[CrossRef\]](#)
- Megahan, W.F.; Molitor, D.C. Erosional effects of wildfire and logging in Idaho. In *Watershed Management Symposium*; American Society of Civil Engineers, Irrigation and Drainage Division: Logan, UT, USA, 1975; pp. 423–444.
- Shakesby, R.A.; Doerr, S.H. Wildfire as a hydrological and geomorphological agent. *Earth-Sci. Rev.* **2006**, *74*, 269–307. [\[CrossRef\]](#)
- Parente, J.; Girona-García, A.; Lopes, A.R.; Keizer, J.J.; Vieira, D.C.S. Prediction, validation, and uncertainties of a nation-wide post-fire soil erosion risk assessment in Portugal. *Sci. Rep.* **2022**, *12*, 2945. [\[CrossRef\]](#)
- Depoutis, N.; Michalopoulou, M.; Kavoura, K.; Nikolakopoulos, K.; Sabatakakis, N. Estimating Soil Erosion Rate Changes in Areas Affected by Wildfires. *ISPRS Int. J. Geo-Inf.* **2020**, *9*, 562. [\[CrossRef\]](#)
- Myronidis, D.; Emmanouloudis, D.; Mitsopoulos, I.; Riggos, E. Soil Erosion Potential after Fire and Rehabilitation Treatments in Greece. *Environ. Modeling Assess.* **2010**, *15*, 239–250. [\[CrossRef\]](#)
- Efthimiou, N.; Psomiadis, E.; Panagos, P. Fire severity and soil erosion susceptibility mapping using multi-temporal Earth Observation data: The case of Mati fatal wildfire in Eastern Attica, Greece. *CATENA* **2020**, *187*, 104320. [\[CrossRef\]](#)
- Kastridis, A.; Kamperidou, V. Evaluation of the post-fire erosion and flood control works in the area of Cassandra (Chalkidiki, North Greece). *J. For. Res.* **2015**, *26*, 209–217. [\[CrossRef\]](#)

17. Richter, G. Aspects and problems of soil erosion hazard in the EEC countries. In *Soil Erosion*; Prendergast, A.G., Ed.; Commission of the European Communities: Report No. EUR 8427 EN; Office for Official Publications of the European Communities: Luxembourg, 1983; pp. 9–17.
18. Rulli, M.C.; Rosso, R. Modeling catchment erosion after wildfires in the San Gabriel Mountains of Southern California. *Geophys. Res. Lett.* **2005**, *32*, 1–4. [[CrossRef](#)]
19. Fernández, C.; Vega, J.A.; Vieira, D.C.S. Assessing soil erosion after fire and rehabilitation treatments in NW Spain: Performance of RUSLE and revised Morgan-Morgan-Finney models. *Land Degrad. Dev.* **2010**, *21*, 58–67. [[CrossRef](#)]
20. Varela, M.E.; Benito, E.; Keijer, J.J. Wildfire effects on soil erodibility of woodlands in NW Spain. *Land Degrad. Dev.* **2010**, *21*, 75–82. [[CrossRef](#)]
21. Moody, J.A.; Shakesby, R.A.; Robichaud, P.R.; Cannon, S.H.; Martin, D.A. Current research issues related to post-wildfire runoff and erosion processes. *Earth Sci. Rev.* **2013**, *122*, 10–37. [[CrossRef](#)]
22. Evans, R. Factors controlling soil erosion and runoff and their impacts in the upper Wissey catchment, Norfolk, England: A ten year monitoring programme. *Earth Surf. Processes Landf.* **2017**, *42*, 2266–2279. [[CrossRef](#)]
23. Karalis, S.; Karymbalis, E.; Mamassis, N. Models for sediment yield in mountainous Greek catchments. *Geomorphology* **2018**, *322*, 76–88. [[CrossRef](#)]
24. Shakesby, R.A. Post-wildfire soil erosion in the Mediterranean: Review and future research directions. *Earth-Sci. Rev.* **2011**, *105*, 71–100. [[CrossRef](#)]
25. Fernández, C.; Vega, J.A. Evaluation of RUSLE and PESERA models for predicting soil erosion losses in the first year after wildfire in NW Spain. *Geoderma* **2016**, *273*, 64–72. [[CrossRef](#)]
26. Tselka, I.; Krassakis, P.; Rentzelos, A.; Koukouzas, N.; Parcharidis, I. Assessing Post-Fire Effects on Soil Loss Combining Burn Severity and Advanced Erosion Modeling in Malesina, Central Greece. *Remote Sens.* **2021**, *13*, 5160. [[CrossRef](#)]
27. Prats, S.A.; González-Pelayo, O.; Silva, F.S.; Bokhorst, K.J.; Baartman, J.E.M.; Keizer, J.J. Post-fire soil erosion reduction with forest residue mulching at catchment scale. *Earth Surf. Processes Landf.* **2019**, *44*, 2837–2848. [[CrossRef](#)]
28. Girona-García, A.; Vieira, D.; Silva, J.; Fernández, C.; Robichaud, P.; Keizer, J. Effectiveness of post-fire soil erosion mitigation treatments: A systematic review and meta-analysis. *Earth-Sci. Rev.* **2021**, *217*, 103611. [[CrossRef](#)]
29. Das, D. Identification of Erosion Prone Areas by Morphometric Analysis Using GIS. *J. Inst. Eng. India Ser. A* **2014**, *95*, 61–74. [[CrossRef](#)]
30. Singh, W.R.; Barman, S.; Tirkey, G. Morphometric analysis and watershed prioritization in relation to soil erosion in Dudhnaï Watershed. *Appl. Water Sci.* **2021**, *11*, 151. [[CrossRef](#)]
31. Vafeidis, A.T.; Drake, N.A.; Wainwright, J. A proposed method for modelling the hydrologic response of catchments to burning with the use of remote sensing and GIS. *CATENA* **2007**, *70*, 396–409. [[CrossRef](#)]
32. Polykretis, C.; Alexakis, D.D.; Grillakis, M.G.; Agapiou, A.; Cuca, B.; Papadopoulos, N.; Sarris, A. Assessment of water-induced soil erosion as a threat to cultural heritage sites: The case of Chania prefecture, Crete Island, Greece. *Big Earth Data* **2021**. [[CrossRef](#)]
33. Benzougagh, B.; Meshram, S.G.; Dridri, A.; Boudad, L.; Baamar, B.; Sadkaoui, D.; Khedher, K.M. Identification of critical watershed at risk of soil erosion using morphometric and geographic information system analysis. *Appl. Water Sci.* **2022**, *12*, 8. [[CrossRef](#)]
34. Rulli, C.M.; Offeddu, L.; Santini, M. Modeling post-fire water erosion mitigation strategies,” *Hydrology and Earth System. Science* **2012**, *17*, 2323–2337. [[CrossRef](#)]
35. Samela, C.; Imbrenda, V.; Coluzzi, R.; Pace, L.; Simoniello, T.; Lanfredi, M. Multi-Decadal Assessment of Soil Loss in a Mediterranean Region Characterized by Contrasting Local Climates. *Land* **2022**, *11*, 1010. [[CrossRef](#)]
36. Saha, S.; Gayen, A.; Pourghasemi, H.R.; Tiefenbacher, J.P. Identification of soil erosion-susceptible areas using fuzzy logic and analytical hierarchy process modeling in an agricultural watershed of Burdwan district, India. *Environ. Earth Sci.* **2019**, *78*, 649. [[CrossRef](#)]
37. Sinshaw, B.G.; Belete, A.M.; Tefera, A.K.; Dessie, A.B.; Bizuneh, B.B.; Alem, H.T.; Atanaw, S.B.; Eshete, D.G.; Wubetu, T.G.; Atinkut, H.B.; et al. Prioritization of potential soil erosion susceptibility region using fuzzy logic and analytical hierarchy process, upper Blue Nile Basin, Ethiopia. *Water-Energy Nexus* **2021**, *4*, 10–24. [[CrossRef](#)]
38. Borrelli, P.; Märker, M.; Panagos, P.; Schütt, B. Modeling soil erosion and river sediment yield for an intermountain drainage basin of the Central Apennines, Italy. *CATENA* **2014**, *114*, 45–58. [[CrossRef](#)]
39. Phinzi, K.; Ngetar, N.S. The assessment of water-borne erosion at catchment level using GIS-based RUSLE and remote sensing: A review. *Int. Soil Water Conserv. Res.* **2019**, *7*, 27–46. [[CrossRef](#)]
40. Brini, I.; Alexakis, D.D.; Kalaitzidis, C. Linking Soil Erosion Modeling to Landscape Patterns and Geomorphometry: An Application in Crete, Greece. *Appl. Sci.* **2021**, *11*, 5684. [[CrossRef](#)]
41. Giambastiani, Y.; Giusti, R.; Gardin, L.; Cecchi, S.; Iannuccilli, M.; Romanelli, S.; Bottai, L.; Ortolani, A.; Gozzini, B. Assessing Soil Erosion by Monitoring Hilly Lakes Silting. *Sustainability* **2022**, *14*, 5649. [[CrossRef](#)]
42. Van Andel, T.H.; Zangger, E.; Demitrac, A. Land Use and Soil Erosion in Prehistoric and Historical Greece. *J. Field Archaeol.* **1990**, *17*, 379–396. [[CrossRef](#)]
43. Zangger, E. Neolithic to Present Soil Erosion in Greece. In *Past and Present Soil Erosion, Archaeological and Geographical Perspectives (Oxbow Monograph 22)*, 1st ed.; Bell, M., Boardman, J., Eds.; Oxford Books: Oxford, UK, 1992; pp. 133–147.

44. Koutalakis, P.; Zaimis, G.N.; Iakovoglou, V.; Ioannou, K. Reviewing Soil Erosion in Greece, World Academy of Science, Engineering and Technology. *Int. J. Geol. Environ. Eng.* **2015**, *9*, 936–941. [[CrossRef](#)]
45. Schismenos, S.; Emmanouloudis, D.; Stevens, G.J.; Katopodes, N.D.; Melesse, A.M. Soil governance in Greece: A snapshot. *Soil Secur.* **2022**, *6*, 100035. [[CrossRef](#)]
46. Rozos, D.; Skilodimou, H.D.; Loupasakis, C.; Bathrellos, G.D. Application of the revised universal soil loss equation model on landslide prevention. An example from N. Euboea (Evia) Island, Greece. *Environ Earth Sci.* **2013**, *70*, 3255–3266. [[CrossRef](#)]
47. Evelpidou, N.; Tzouxanioti, M.; Gavalas, T.; Spyrou, E.; Saitis, G.; Petropoulos, A.; Karkani, A. Assessment of Fire Effects on Surface Runoff Erosion Susceptibility: The Case of the Summer 2021 Forest Fires in Greece. *Land* **2022**, *11*, 21. [[CrossRef](#)]
48. Wischmeier, W.H.; Smith, D.D. *Predicting Rainfall Erosion Losses. A Guide to Conservation Planning*; Agriculture Handbook No.537; United States Department of Agriculture, Science and Education Administration: Hyattsville, MD, USA, 1978; p. 62.
49. Roberts, S.; Jackson, J. Active normal faulting in central Greece: An overview. In *The Geometry of Normal Faults*; Roberts, A.M., Yielding, G., Freeman, B., Eds.; Geological Society, Special Publications: London, UK, 1991; Volume 56, pp. 125–142.
50. Valkanou, K.; Karymbalis, E.; Papanastassiou, D.; Soldati, M.; Chalkias, C.; Gaki-Papanastassiou, K. Morphometric Analysis for the Assessment of Relative Tectonic Activity in Evia Island, Greece. *Geosciences* **2020**, *10*, 264. [[CrossRef](#)]
51. Valkanou, K.; Karymbalis, E.; Papanastassiou, D.; Soldati, M.; Chalkias, C.; Gaki-Papanastassiou, K. Assessment of Neotectonic Landscape Deformation in Evia Island, Greece, Using GIS-Based Multi-Criteria Analysis. *ISPRS Int. J. Geo-Inf.* **2021**, *10*, 118. [[CrossRef](#)]
52. Mountrakis, D.M. *Geology of Greece*; University Studio Press: Thessaloniki, Greece, 1985. (In Greek)
53. Mariolopoulos, E.G. *The Climate of Greece*; Academy of Athens Research Center for Atmospheric Physics and Climatology: Athens, Greece, 1938; No. 7; pp. 79–82.
54. Mariolopoulos, H.G. *Compendium of the Climate of Greece*; KEFAK of the Academy of Athens: Athens, Greece, 1982; No. 7; pp. 9–76.
55. Zerefos, C.; Repapis, C.; Giannakopoulos, C.; Kapsomenakis, J.; Papanikolaou, D.; Papanikolaou, M.; Poulos, S.; Vrekoussis, M.; Philandras, C.; Tselioudis, G.; et al. The climate of the Eastern Mediterranean and Greece: Past, present and future. In *The Environmental, Economic and Social Impacts of Climate Changing Greece*; Bank of Greece: Athens, Greece, 2011; pp. 50–58.
56. Giannaros, T.M.; Papavasileiou, G.; Lagouvardos, K.; Kotroni, V.; Dafis, S.; Karagiannidis, A.; Dragozi, E. Meteorological Analysis of the 2021 Extreme Wildfires in Greece: Lessons Learned and Implications for Early Warning of the Potential for Pyroconvection. *Atmosphere* **2022**, *13*, 475. [[CrossRef](#)]
57. Gemitzi, A.; Koutsias, N. A Google Earth Engine code to estimate properties of vegetation phenology in fire affected areas—A case study in North Evia wildfire event on August 2021. *Remote Sens. Appl. Soc. Environ.* **2022**, *26*, 100720. [[CrossRef](#)]
58. Copernicus Emergency Management Service Mapping (EMS). Available online: <https://emergency.copernicus.eu/mapping/ems/forest-fire-evia-island-greece-1> (accessed on 7 September 2022).
59. Mwansa, P. Investigating the Impact of Fire on the Natural Regeneration of Woody Species in Dry and Wet Miombo Woodland. Master’s Thesis, Faculty of AgriSciences, Stellenbosch University, Stellenbosch, South Africa, 2018.
60. Van der Knijff, J.; Jones, R.; Montanarella, L. *Soil Erosion Risk Assessment in Europe*; European Soil Bureau, Joint Research Centre EUR 19044 EN: Brussels, Belgium, 2000.
61. Kolli, M.K.; Opp, C.; Groll, M. Estimation of soil erosion and sediment yield concentration across the Kolleru Lake catchment using GIS. *Env. Earth Sci.* **2021**, *80*, 161. [[CrossRef](#)]
62. Bathrellos, G.; Skilodimou, H.; Chousianitis, K. Soil Erosion Assessment in Southern Evia Island Using USLE and GIS. *Bull. Geol. Soc. Greece* **2010**, *43*, 1572–1581. [[CrossRef](#)]
63. Moore, I.D.; Turner, A.K.; Wilson, J.P.; Jenson, S.K.; Band, L.E. GIS and land-surface-subsurface process modeling. In *Environmental Modeling with GIS*; Goodchild, M.F.R., Parks, B.O., Steyaert, L.T., Eds.; Oxford University Press: Oxford, UK, 1993; pp. 196–230.
64. Bathrellos, G.D.; Skilodimou, H.D.; Chousianitis, K.; Youssef, A.M.; Pradhan, B. Suitability estimation for urban development using multi-hazard assessment map. *Sci. Total Env.* **2017**, *575*, 119–134. [[CrossRef](#)]
65. Skilodimou, H.D.; Bathrellos, G.D.; Alexakis, D.E. Flood Hazard Assessment Mapping in Burned and Urban Areas. *Sustainability* **2021**, *13*, 4455. [[CrossRef](#)]
66. Bathrellos, G.D.; Skilodimou, H.D. Land Use Planning for Natural Hazards. *Land* **2019**, *8*, 128. [[CrossRef](#)]